

RSC Advances



This is an *Accepted Manuscript*, which has been through the Royal Society of Chemistry peer review process and has been accepted for publication.

Accepted Manuscripts are published online shortly after acceptance, before technical editing, formatting and proof reading. Using this free service, authors can make their results available to the community, in citable form, before we publish the edited article. This *Accepted Manuscript* will be replaced by the edited, formatted and paginated article as soon as this is available.

You can find more information about *Accepted Manuscripts* in the [Information for Authors](#).

Please note that technical editing may introduce minor changes to the text and/or graphics, which may alter content. The journal's standard [Terms & Conditions](#) and the [Ethical guidelines](#) still apply. In no event shall the Royal Society of Chemistry be held responsible for any errors or omissions in this *Accepted Manuscript* or any consequences arising from the use of any information it contains.

Cite this: DOI: 10.1039/c0xx00000x

www.rsc.org/xxxxxx

ARTICLE TYPE

Optically active helical polyacetylene/Fe₃O₄ composite microspheres: prepared by precipitation polymerization and used for enantioselective crystallization

Huaiyu Chen,^{a,b} Lei Li,^{a,b,c} Dong Liu,^{a,b} Huajun Huang,^{a,b} Jianping Deng*^{a,b} and Wantai Yang^{a,b}

5 Received (in XXX, XXX) Xth XXXXXXXXXX 20XX, Accepted Xth XXXXXXXXXX 20XX

DOI: 10.1039/b000000x

The article reports the first coordination-precipitation polymerizations for preparing chiral, magnetic composite microspheres consisting of helical substituted polyacetylene and Fe₃O₄ nanoparticles. The microspheres were obtained in high yield (>85%) and characterized by XRD, FT-IR, SEM, TEM, CD and UV-vis absorption techniques. TEM and SEM images showed that the microspheres were approx. 600 nm in average diameter and possessed spheric morphology with rough surface. CD and UV-vis absorption spectra demonstrated that the polyacetylene chains constructing the microspheres adopted helical structures of predominantly one handed screw sense, which enabled the microspheres to show remarkable optical activity. The microspheres also performed desirable magneticity. They were further used as chiral selectors efficiently inducing enantioselective crystallization of D- and L-alanine as model chiral enantiomers. Moreover, the microspheres can be easily restored under the assistance of an external magnetic field. The coordination-precipitation polymerizations provide a versatile platform for preparing advanced chiral and non-chiral, magnetic hybrid microspheres.

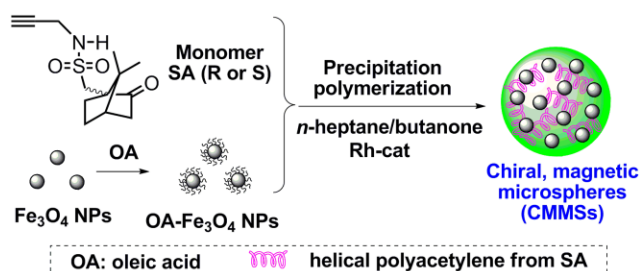
1. Introduction

Chiral helical polymers have attracted increasing attention in polymer science because of their intriguing helical structures and optical activity which cannot be observed in ordinary polymers. This unique type of polymers have been extensively investigated in significant research areas such as chiral recognition/resolution, asymmetry catalysis, enantioselective crystallization, etc.¹⁻⁷ Chiral helical polymers are interesting also for the “chiral amplification” effect.^{8,9} So far a variety of artificial helical polymers have been elegantly designed and synthesized accordingly.¹⁰⁻¹⁶ Among the synthesized helical polymers, substituted polyacetylenes have gathered special attention due to their typically conjugated polymer main chains adopting helical conformations and the pendant groups providing the desired functionality.^{17,18} More recently, optically active nano- and micro-spheres were fabricated based on helical substituted polyacetylenes as a newly emerging class of advanced materials.^{17,19,20} The intriguing spheres can be prepared by diverse methods, including emulsion polymerization,¹⁹ seed emulsion polymerization,²⁰ suspension polymerization,²¹ self-assembly,²² and precipitation polymerization²³ approaches. Among the methods, precipitation polymerization shows pronounced advantages due to the relatively facile operation, simple polymerization system, and pure polymer spheres. Therefore precipitation polymerization technique was particularly established by us for preparing optically active polymer spheres constructed by helical polyacetylenes.²³ The as-prepared polymer

spheres were successfully utilized as specific “chiral selectors” for inducing enantioselective crystallization of racemates.^{20,23} Nonetheless, such spheres also showed an intractable disadvantage in terms of recycling. To overcome this limitation, we prepared optically active, magnetic composite particles (OAMCPs) by using suspension polymerization technique.²⁴ The OAMCPs could be conveniently recycled with the help of an external magnetic field. Unfortunately, suspension polymerization required a large amount of stabilizer, which in turn resulted in another problem, i.e. how to entirely exclude the residual stabilizer in the produced spheres. To solve the problem and to further enrich the types of chiral polymer spheres, we in the present study successfully established a facile but efficient coordination-precipitation polymerization methodology, by which pure chiral magnetic microspheres can be fabricated with much ease.

Magnetic spheres have attracted large interest from diverse research fields of physics, chemistry, materials, and biomedicine.²⁵ Composite spheres simultaneously combining magneticity with other interesting properties for instance electric,²⁶ thermal,²⁷ catalytic,²⁸ fluorescent²⁹ properties currently gather ever-growing attention. The thus-obtained composite spheres are expected to find uses in magnetic resonance imaging,^{30,31} catalysis,^{29,32} separation,³³ drug delivery and release.^{34,35} Chiral, magnetic composite spheres are relatively new advanced functional materials, which judiciously combine both magnetic property and optical activity. They have found significant applications especially in chiral-related areas. Some groups^{29,36,37} elegantly immobilized chiral catalysts on magnetic

spheres and applied them in asymmetric catalyses. More remarkably, the spheres could be magnetically recycled and reused for several times. $\text{Fe}_3\text{O}_4@/\text{SiO}_2$ particles were chirally functionalized by using chiral selectors, which were utilized in chiral separation processes.^{38,39} Up to date nearly all the chiral magnetic spheres were constructed by using chiral small molecules or biomacromolecules.^{40,41} As mentioned above, optically active helical polymers possess “chiral amplification” feature.^{8,9} Accordingly, we prepared optically active, magnetic Fe_3O_4 -polystyrene-polyacetylene composite microspheres,²⁴ by integrating “macromolecular helicity-derived chirality” and “magnetism” in one single microsphere entity. Nevertheless, these microspheres suffer from disadvantages including tedious preparative procedure and complex components. Thus a more straightforward approach is still required to simplify the preparation process, while keeping the favorable properties (in particular both optical activity and magnetism) of the microspheres.



Scheme 1 Schematic illustration of preparing chiral, magnetic microspheres (CMMSSs) by coordination-precipitation polymerization.

In the above context, we in the present study designed and successfully prepared a novel class of chiral, magnetic microspheres (abbreviated as CMMSSs) by using a straightforward one-pot coordination-precipitation polymerization approach (**Scheme 1**). The major objectives include: (1) To establish a new, straightforward, and effective technique, i.e. precipitation polymerization of substituted acetylene monomer in the presence Fe_3O_4 nanoparticles (NPs), for preparing pure chiral magnetic microspheres (CMMSSs). (2) To use the obtained CMMSSs as chiral additive to accomplish enantioselective crystallization.

2. Experimental Section

2.1 Measurements

Fourier transform infrared (FT-IR) spectra were performed on a Nicolet NEXUS 670 spectrophotometer (KBr tablet). Powder X-ray diffraction (XRD) patterns were obtained using a D/max2500 VB2+/PC X-ray diffractometer (Rigaku) using Cu K radiation. Transmission electron microscopy (TEM) images were observed using a JEM-2100 (JEOL) transmission electron microscope at an accelerating voltage of 200 kV. The structure and morphology of the microspheres were observed on a Zeiss SUPRA 55 scanning electron microscope (SEM) equipped with an energy-dispersive X-ray (EDX) detector. Circular dichroism (CD) and UV-vis absorption spectra were recorded using a JASCO J-810 spectropolarimeter. Specific rotations were measured on a JASCO P-1020 digital polarimeter with a sodium lamp as the light source at room temperature. Thermogravimetric analysis

(TGA) was carried out with a Q50 TGA at a scanning rate of 10 °C/min in air. Magnetic property was measured using a vibrating sample magnetometer (VSM, Lake Shore 7410 VSM) at room temperature. ¹H NMR spectra were recorded on a Bruker AV 400 spectrometer. The molecular weights and molecular weight polydispersities were determined by GPC (Waters 515-2410 system) calibrated by using polystyrenes, with THF as eluent. Raman spectra were obtained with a microscopic confocal Raman spectrometer spectrophotometer (Renishaw).

2.2 Materials

$\text{FeCl}_3 \cdot 6\text{H}_2\text{O}$, $\text{FeSO}_4 \cdot 7\text{H}_2\text{O}$, $\text{NH}_3 \cdot \text{H}_2\text{O}$ (28%), anhydrous ethanol, chloroform (CHCl_3), tetrahydrofuran (THF), butanone, *n*-heptane, ethyl acetate, anhydrous MgSO_4 , hydrochloric acid (HCl), and oleic acid (OA) (all analytic grade) were purchased from Beijing Chemical Reagents Company (China) and used as received. Propargylamine, isobutyl chloroformate, 4-methylmorpholine, 1S-(+)- and 1R-(-)-camphorsulfonyl chloride were brought from Alfa Aesar and used without further purification. $(\text{nbdrh})\text{Rh}^+\text{B}^-(\text{C}_6\text{H}_5)_4$ was prepared in the way reported earlier.⁴² Substituted acetylene monomers (SA monomers including both R- and S-SA, structurally presented in Scheme 1) were synthesized according to the previous study.⁴³ D- and L-alanine were purchased from Aladdin Reagent Co. (Shanghai, China). They were used without additional purification. Freshly deionized water was used in the whole study.

2.3 Preparation of oleic acid (OA) modified Fe_3O_4 nanoparticles (NPs)

The oleic acid modified Fe_3O_4 (OA- Fe_3O_4) NPs were prepared according to the method reported in literature.⁴⁴ The procedure includes two major steps, as briefly described below. Firstly, Fe_3O_4 NPs were prepared by co-precipitation method. 2.35 g $\text{FeSO}_4 \cdot 7\text{H}_2\text{O}$ and 4.1 g $\text{FeCl}_3 \cdot 6\text{H}_2\text{O}$ were dissolved in 100 mL deionized water. After stirring for 20 minutes under N_2 , ammonium hydroxide (25 mL) was quickly injected into the reaction mixture at room temperature. Magnetic NPs was immediately formed as black precipitate. Then the reaction temperature was heated to 80 °C. Secondly, oleic acid (1 mL) was slowly added into the above solution within 1 hour. The whole process was performed under N_2 protection. The reaction continued for another 1 hour. After cooling to room temperature, 0.5 g NaCl was added in the mixture solution. Then the OA- Fe_3O_4 NPs were extracted from the above solution by using toluene, obtaining OA- Fe_3O_4 NPs dispersion. The toluene in the OA- Fe_3O_4 NPs dispersion was evaporated and the OA- Fe_3O_4 NPs were re-dispersed in *n*-heptane (20 mg/mL) for the subsequent uses.

2.4 Fabrication of chiral magnetic composite microspheres (CMMSSs)

The composite microspheres were prepared by precipitation polymerization method, referring to the precipitation polymerization approach established by us earlier.²³ A typical preparative process is briefly introduced below. One of the SA monomers (R- or S-SA, Scheme 1) was added in a glass tube equipped with a three-way stopcock under nitrogen, while Rh catalyst was charged in another tube. The two tubes were separately degassed with N_2 . Then, 0.5 mL of butanone was

added into each tube to dissolve the monomer and catalyst. Afterwards, the Rh catalyst solution was transferred into the monomer solution, and then 9 mL of the OA-Fe₃O₄/*n*-heptane dispersion prepared above was immediately added into the solution. The whole process was performed under N₂. The polymerization was performed at 30 °C for 3 h. After the completion of polymerization, CMMSSs were formed. We totally prepared four groups of CMMSSs, for which the main parameters are illustrated in Table 1.

Table 1 Parameters for preparing CMMSSs-1~CMMSSs-4.

CMMSSs	Monomer (mmol)	[Rh]:[M] (mol/mol)	OA-Fe ₃ O ₄ ^a (wt%)	Yield ^b (wt%)
CMMSSs-1	(<i>S</i>)-SA,0.5	1/100	10	90.5
CMMSSs-2	(<i>R</i>)-SA,0.5	1/100	10	91.3
CMMSSs-3	(<i>S</i>)-SA,0.5	1/100	20	85.5
CMMSSs-4	(<i>S</i>)-SA,0.5	1/100	30	89.7

^a The weight ratio of OA-Fe₃O₄ NPs to monomer.

^b The yield of CMMSSs.

2.5 Enantioselective crystallization

Enantioselective crystallization with D- and L-alanine as chiral enantiomers was performed as briefly stated below, according to the studies by Mastai^{45,46} and us.²⁰ All the crystallization processes were carried out from supersaturated solutions of racemic alanine in deionized water. 270 mg of D- and L-alanine were added in deionized water (approx. 3 mL) and the solution was heated to 35 °C and stirred till complete dissolution. A predetermined amount of the CMMSSs was charged in the racemic D,L-alanine supersaturated aqueous solution and then stirred for about 15 min. The solution was cooled spontaneously to approx. 25 °C, during which crystals appeared. The crystals were filtrated after crystallization lasting for about 72 hours. Induced alanine crystals and residual alanine solution were separated by filtration. The dried crystals were subjected to SEM, XRD and CD spectroscopy measurements. More detailed crystallization processes were described in our previous studies.^{20,47}

The samples for CD spectroscopy measurements were prepared as follows: the induced alanine crystals were added in deionized water (approx. 3 mL). Residual alanine solution and the CMMSSs were separated by a magnet. 270 mg of D- or L-alanine was added in deionized water (approx. 3 mL) to obtain pure alanine enantiomers solution. For the CMMSSs, 0.269 mg of the microspheres were added in ethanol (approx. 10 mL).

3. Results and discussion

3.1 The strategy for preparing CMMSSs

The procedure for preparing chiral magnetic composite microspheres (CMMSSs) is schematically presented in Scheme 1. The typical procedure comprises two steps: (1) Fe₃O₄ NPs were prepared by co-precipitation approach and then modified with oleic acid as earlier reported.²⁴ (2) The CMMSSs were prepared via coordination-precipitation polymerization of acetylene monomer (SA) by using (nbd)Rh⁺B⁻(C₆H₅)₄ as catalyst in the presence of OA-Fe₃O₄ NPs. The process is detailed in Experimental section. The as-prepared CMMSSs possessed simultaneously both magnetic responsivity and optical activity, respectively resulting from Fe₃O₄ NPs and helical polymer chains with predominantly one-handed helicity. Herein it should be

pointed out that oleophilic OA-Fe₃O₄ NPs can be homogeneously dispersed in *n*-heptane, by which we could prepare the designed chiral magnetic microspheres. When pure Fe₃O₄ NPs were used instead of OA-Fe₃O₄ NPs, regular microspheres could not be formed due to the easy aggregation of the Fe₃O₄ NPs. To acquire deeper insights into the novel CMMSSs, we also prepared CMMSSs with varied magnetic content (OA-Fe₃O₄ NPs), as presented in Table 1.

3.2 Primary characterizations of CMMSSs

Fe₃O₄ magnetic nanoparticles (Fe₃O₄ NPs) can be prepared by diverse approaches, including thermo-decomposition,⁴⁸ chemical co-precipitation,⁴⁹ solvothermal method,⁵⁰ etc. In our study, we took the relatively simple chemical co-precipitation way to prepare OA-Fe₃O₄ NPs. The as-prepared OA-Fe₃O₄ NPs could be well dispersed in organic solvent, as shown in **Figure 1A**. The average diameter of the OA-Fe₃O₄ NPs was ca. 13 nm according to TEM image.

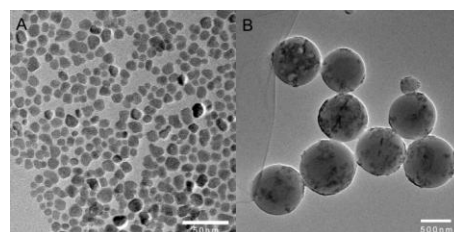


Fig. 1 Typical TEM images of OA-Fe₃O₄ NPs (A) and CMMSSs (B) (taking CMMSSs-1 in Table 1 as example).

In the preceding study, we prepared optically active spheres derived from helical substituted polyacetylene by using coordination-precipitation polymerization.²³ We found that suitable solvent mixture played key roles in performing precipitation polymerization of substituted acetylene monomers. A mixture solvent of butanone/*n*-heptane with the ratio of 1/9 (v/v) favorably provided microspheres consisting of optically active helical substituted polyacetylene. Herein by taking the mixture solvent of butanone/*n*-heptane (1/9, v/v; The former serves as good solvent, while the latter as poor solvent.), we further successfully prepared the anticipated CMMSSs. A typical TEM image of the CMMSSs is presented in Figure 1B, taking CMMSSs-1 as example (see Table 1). From the TEM image, spherical microspheres were fabricated with an average diameter of ca. 600 nm. In addition, the OA-Fe₃O₄ NPs (the dark parts) can also be clearly observed in the CMMSSs (Figure 1B). The obtained CMMSSs were further observed by SEM, as presented in **Figure 2**. The microspheres exhibited rough surfaces due to the presence of Fe₃O₄ NPs.

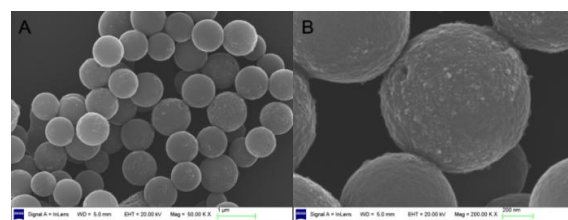


Fig. 2 Typical SEM images of CMMSSs-1 (Table 1). The scale bar in (A) 1 μm and (B) 200 nm.

Both the TEM (Figure 1) and SEM (Figure 2) images definitely demonstrate the successful formation of the expected CMMSSs. To further explore the structure and composition of the CMMSSs, they were subsequently characterized by FT-IR, XRD, and TG techniques. The recorded FT-IR spectra of the OA-Fe₃O₄ NPs and the CMMSSs are illustrated in Figure 3. Figure 3A presents the FT-IR spectrum of the OA-Fe₃O₄ NPs, in which the peaks at 2925 and 2856 cm⁻¹ correspond with the C-H stretching vibrations of the alkyl group of oleic acid, evidently confirming that the magnetic NPs were successfully modified by oleic acid. The characteristic peak at 588 cm⁻¹ can also be found, which is ascribed to Fe-O stretching vibration of Fe₃O₄ NPs. A typical FT-IR spectrum of the CMMSSs (CMMSSs-1) is illustrated in Figure 3B, in which new peaks appeared at 3288, 1740, and 1051 cm⁻¹, corresponding to N-H stretching band, C=O stretching vibration of lactone, and camphor group, respectively.^{23,43} The Fe-O stretching vibration of Fe₃O₄ NPs can be observed in the FT-IR spectrum. The FT-IR spectra further supports the conclusion that the microspheres were fabricated as expected.

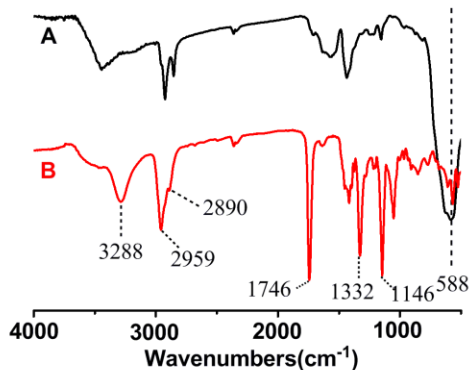


Fig. 3 FT-IR spectra of (A) OA-Fe₃O₄ NPs and (B) CMMSSs-1 (KBr tablet).

Since the CMMSSs were not cross-linked, the polymer chains forming them could be further characterized. GPC measurements indicate that molecular weight (M_n) of the polyacetylene chains constructing the microspheres (take CMMSSs-1 as example) was 3700 and the polydispersity (M_w/M_n) was 1.73. ¹H NMR spectrum of the polymer chains is shown in Figure S1 in Supporting Information (more details are presented therein). In addition to characterizing the structure, ¹H NMR spectroscopy is also highly effective for determining the stereoregularity of substituted polyacetylenes. Referring to a method described previously,⁵¹ the cis content of the polymer chains was 91%. Furthermore, Raman spectrum was also recorded for the polymer chains, as illustrated in Figure S2 in Supporting Information. Based on the integration ratio between the cis C=C and C-C peaks and the trans C=C and C-C peaks in the polymer main chains,⁵² the cis content was determined to be 93%, which is consistent with the value calculated from ¹H NMR spectroscopy (as discussed above). Accordingly, we conclude that the polymer chains forming the CMMSSs possessed high cis content and high stereoregularity, which is favorable for the polymer chains to form helical structures, as reported below.

XRD patterns of OA-Fe₃O₄ NPs and CMMSSs (taking CMMSSs-

1 as representative) were recorded, as illustrated in Figure 4. Diffraction peaks (111), (200), (311), (222), (400), (422), (511), and (440) can be clearly observed in Figure 4A. These diffraction peaks can be indexed as face centered cubic Fe₃O₄ (The Joint Committee on Powder Diffraction Standards (JCPDS) reference (No. 19-0629)). All the diffraction peaks above can be found in the XRD pattern of CMMSSs-1 (Figure 4B) except for the diffraction peak (111). The peak (111) is overlapped by the wide peak at 2θ = 14.8 deg. in Figure 4B. The wide peak (2θ = 14.80 deg.) originated in amorphous polyacetylene.⁵³ The XRD patterns offer a further support for our conclusion. The compositions of the CMMSSs were specifically identified by Energy-dispersive X-ray (EDX) spectra (Figure S3, Supporting Information). EDX analysis of the illuminating electron beams on the surface of the OAMCPs reveals the presence of Fe, C, O, N, and S elements, which indirectly conformed that the microspheres were composed of OA-Fe₃O₄ NPs and substituted polyacetylene.

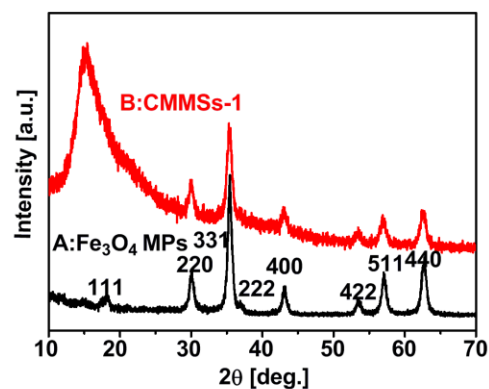


Fig. 4 XRD patterns of (A) OA-Fe₃O₄ NPs and (B) Fe₃O₄-PSA microspheres (CMMSSs-1 as representative).

For magnetic composite microspheres, the magnetic content is one of the key properties of interest. Next we took CMMSSs-1 as representative and characterized them by TGA. The TGA curves of OA-Fe₃O₄ NPs and CMMSSs-1 are presented in Figure 5.

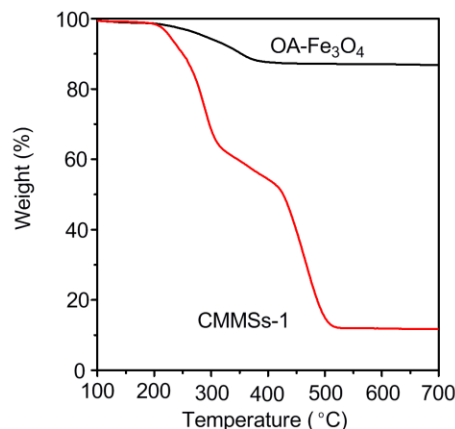


Fig. 5 TGA curves of (A) OA-Fe₃O₄ NPs and (B) CMMSSs-1. Both TGA curves were measured at a scanning rate of 10 °C/min in air.

The TGA curve of oleic acid modified Fe₃O₄ NPs showed a

weight loss of 13.3%. The weight loss was caused by the oleic acid and the transformation from Fe_3O_4 NPs to $\gamma\text{-Fe}_2\text{O}_3$ NPs.⁵⁴ CMMSs-1 showed two pronounced weight loss platforms. The first weight loss occurring at 200–300 °C was caused by oleic acid, polyacetylenes with low molecular weight, and the transformation from Fe_3O_4 NPs to $\gamma\text{-Fe}_2\text{O}_3$ NPs. The second weight loss (400–500 °C) was caused by the polyacetylenes with high molecular weight. The total weight loss is 88.3% when temperature increased from 100 to 700 °C. The magnetic content of the microspheres can be calculated as approx. 12 wt% by the residual $\gamma\text{-Fe}_2\text{O}_3$. This value is accordant with the theoretical one (Table 1).

3.3 Effects of Fe_3O_4 NPs on the morphology of CMMSs

In this study we established a novel, facile, and effective, technique for preparing chiral, magnetic microspheres on the basis of acetylenic monomer and Fe_3O_4 NPs. In the course of precipitation polymerization for forming microspheres, magnetic Fe_3O_4 NPs were found to exert large influence. The content of the magnetic NPs had a great effect on the morphology and property of the resulting microspheres. With the other conditions keeping unchanged, we prepared three sets of CMMSs with varied magnetic contents (Table 1, CMMSs-1, 10 wt%; CMMSs-3, 20 wt%; CMMSs-4, 30 wt% OA- Fe_3O_4 NPs). The SEM images of the three groups of microspheres are displayed in Figure 6. According to the SEM images, the morphology of the CMMSs became unsatisfactory with increasing the content of OA- Fe_3O_4 NPs. Fortunately regular microspheres can be obtained at an appropriate magnetic content (10 wt%, CMMSs-1).

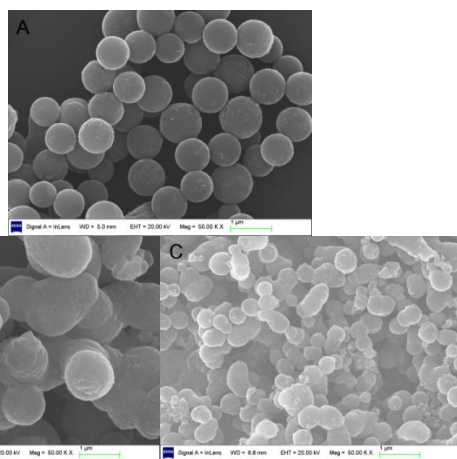


Fig. 6 SEM images of CMMSs: (A) CMMSs-1, 10 wt% OA- Fe_3O_4 ; (B) CMMSs-3, 20 wt% OA- Fe_3O_4 ; (C) CMMSs-4, 30 wt% OA- Fe_3O_4 . The scale bar: 1 μm .

The influence of the OA- Fe_3O_4 NPs on the formation of microspheres can be understood as follows. At the beginning of polymerization, OA- Fe_3O_4 NPs were homogeneously dispersed in the polymerization media. With the polymerization of SA monomer starting and continuing, polymer chains of SA grew longer to a certain length, and then the polymer chains began to precipitate out from the media due to the poor solubility.²³ In this course, the OA- Fe_3O_4 NPs most likely acted as nucleation sites for subsequently forming the composite microspheres, and promoted the formation of microspheres. However, too much OA- Fe_3O_4 NPs seems to be not favorable for the formation of

regular microspheres.

3.4 Optical activity of the CMMSs

Chiral helical polyacetylenes were used to construct the CMMSs under investigation. Our previous studies^{19–24} showed that helical substituted polyacetylenes possessed optical activity, according to circular dichroism (CD) and UV-vis absorption spectroscopies. The optical activity of helical polymer-derived nano- and microspheres was also convincingly characterized by CD and UV-vis spectra analyses in our earlier studies.^{17,19,20} Therefore the present CMMSs were next subjected to CD and UV-vis spectra measurements in dispersion state (dispersed in ethanol), and the obtained spectra are displayed in Figure 7.

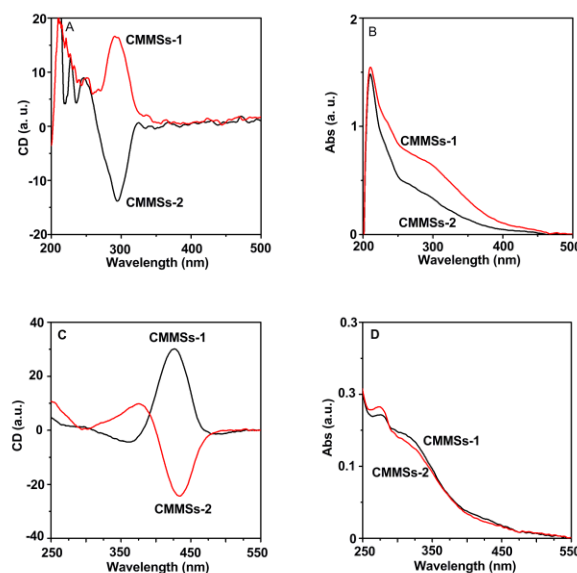


Fig. 7 CD and UV-vis absorption spectra of CMMSs-1 and CMMSs-2 in dispersion (A,B) with ethanol as solvent and solution (C, D) with CHCl_3 as solvent. The spectra were measured at room temperature.

For CMMSs-1 (derived from S-SA, see Table 1), positive CD signals were found around 300 nm, while for CMMSs-2 (derived from R-SA, see Table 1), CD signals with opposite sign were found also around 300 nm (Figure 7A). Corresponding UV-vis absorption occurred at 250–350 nm (Figure 7B). The results demonstrated that the substituted polyacetylene chains constructing the CMMSs adopted helical structures of predominant helicity, according to our earlier intensive studies dealing with optically active nano- and microspheres.^{19–23}

According to the investigations and analyses above, we know that the CMMSs possessed optical activity in dispersion state. In order to further elucidate the helical structures of the acetylenic polymer chains and the optical activity of the microspheres, both CMMSs-1 and CMMSs-2 were dissolved in CHCl_3 and then subjected to CD and UV-vis spectra measurements. Since the microspheres were not crosslinked, they could be easily dissolved in appropriate solvent (e.g. CHCl_3). As expected, the polymer chains forming the microspheres were dissolved, while the Fe_3O_4 NPs were just dispersed in the media. The CD and UV-vis spectra of the solutions are presented in Figure 7(C,D). The helical polyacetylenes (derived from S-SA and R-SA) showed opposite CD signals at 425 nm. Compared to the CD signals (300 nm) in

dispersion state (Figure 7A), the microspheres in dissolved state performed considerable red shift. Similar phenomena were observed in our earlier spheres.^{17,23} The red/blue shifts were caused by the helical polyacetylenes at varied state. In microspheres state, helical polyacetylene chains were condensed, leading to shortened effective conjugation length along the polymer chains. In dissolved state, helical polyacetylene chains extended and their screw pitch increased accordingly. Accordingly, red shift was observed in the dissolved state, as observed in Figure 7C. For UV-vis absorption spectra (Figure 7D), further useful information could not be acquired due to the complex situation of the samples.

3.5 Magnetic property of the CMMSs

The currently investigated CMMSs were also expected to show magnetism. The magnetic properties of the OA-Fe₃O₄ NPs and CMMSs were investigated by using a VSM, and the results are shown in Figure 8, taking CMMSs-1 as representative. Figure 8A shows the hysteresis loop of the OA-Fe₃O₄ NPs, indicating that the maximum saturation magnetization (MSM) was 69.8 emu/g. The hysteresis loop of CMMSs-1 is displayed in Figure 8B. The MSM reduced to 7.1 emu/g (CMMSs-1, 10 wt% OA-Fe₃O₄). Compared to OA-Fe₃O₄ NPs, the MSM of CMMSs-1 drastically decreased because of the presence of non-magnetic polyacetylene. Nonetheless, the low MSM still enabled the microspheres to be responsive to external magnetic field.

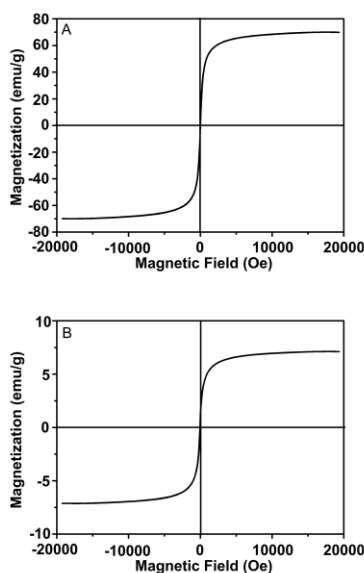


Fig. 8 Hysteresis loops of (A) OA-Fe₃O₄ NPs and (B) CMMSs-1 at room temperature.

The magnetic responsivity of CMMSs-1 was further experimentally verified by utilizing a magnet, as can be seen in Figure 9. Figure 9 shows that the time from dispersion state (A) to aggregation state (B) was completed within 15 seconds. Furthermore, state (B) returned to state (A) again when the magnet was taken away. This remarkable magnetic responsivity rendered the CMMSs with recycling ability, which is especially desirable for practical applications.

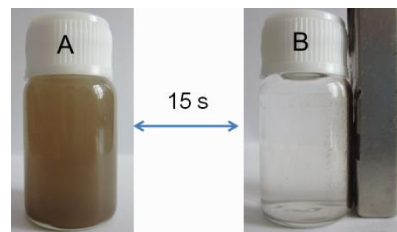


Fig. 9 The responsiveness of CMMSs-1 to external magnetic field. The dispersion state (A) transitioned to aggregation state (B) within 15 seconds.

3.6 Enantioselective crystallization with CMMSs

In previous studies, we prepared chiral polymer nanospheres²³ and even chiral nanospheres with two-layered hollow structures²⁰ based on helical substituted polyacetylenes. Both the two types of chiral spheres efficiently induced enantioselective crystallization. To further improve the dispersibility of the chiral nanospheres, they were immobilized covalently on oxide graph (GO) to fabricate a novel category of chiralized GO derivatives,⁴⁷ which also effectively induced enantioselective crystallization. Nonetheless, all the processes above showed an intractable problem, i.e. the tedious and troublesome process for isolating the chiral spheres from the crystals and the residual racemic solution. To further overcome the problem, we in the present study designed and prepared chiral, magnetic nanospheres, aiming to simplify the recycling of the nanospheres by taking advantage of the magnetism.

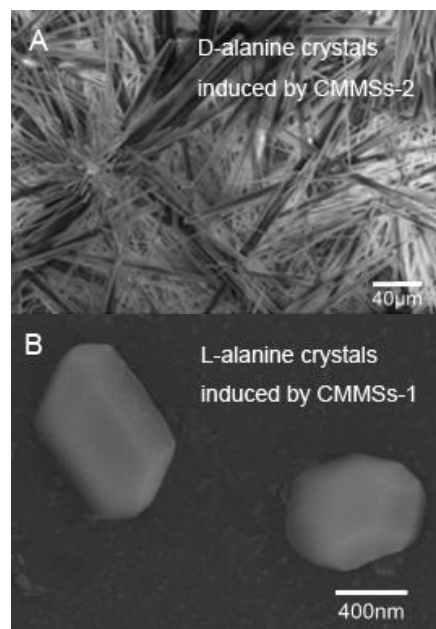


Fig. 10 SEM images of D-alanine crystals by using CMMSs-2 ((R)-PSA microspheres) (A, ee 79%) and L-alanine crystals by using CMMSs-1 ((S)-PSA microspheres) (B, ee 62%).

The resulting chiral magnetic microspheres were subsequently used as specific chiral selectors toward enantioselective crystallization. Taking alanine as example, the induced crystals are presented in Figure 10, by using CMMSs-1 (derived from S-SA) and CMMSs-2 (derived from R-SA) as specific chiral selectors. SEM images showed two kinds of crystals, needle-like (Figure 10A) and octahedral (Figure 10B) crystals. To further elucidate the crystals, we measured their CD spectra, together

with the pure alanine enantiomers. In this study, we employed two monomers (S- and R-SA, Scheme 1 and Table 1) to fabricate the two kinds of chiral magnetic microspheres, i.e. CMMSs-1 ((S)-PSA-based microspheres) and CMMSs-2 ((R)-PSA-based microspheres) (see Table 1). Apart from the induced alanine crystals, pure alanine enantiomers, the CMMSs, and the corresponding residual alanine solutions after crystallization were all characterized by CD spectroscopy. All the recorded CD spectra are illustrated in **Figure 11**.

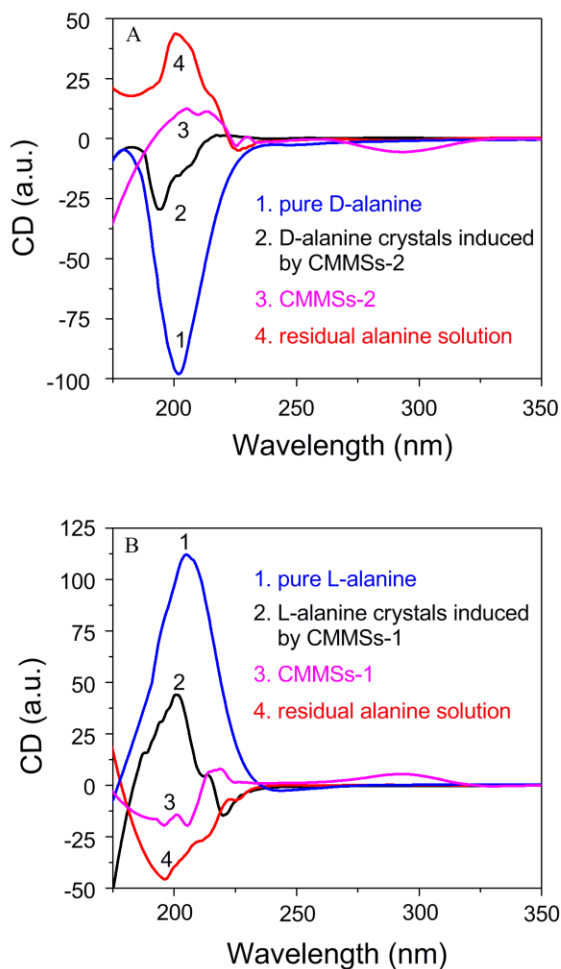


Fig. 11 CD spectra of the induced alanine crystals by using (A) CMMSs-2 and (B) CMMSs-1. All the spectra were recorded at room temperature. For CD spectra measurement, CMMSs-1 and CMMSs-2 were dispersed in ethanol; the other samples were dissolved in deionized water.

In Figure 11, all the alanine solutions showed intense CD signal around 200 nm, while the CMMSs showed the expected CD signal around 300 nm, just like Figure 7A. A combination of the SEM images of the crystals (Figure 10) and the CD spectra (Figure 11) reveals that CMMSs-2, i.e. (R)-PSA-based microspheres, majorly induced D-alanine to form needle-like crystals with ee (enantiomeric excess) of 79% (Figure 10A). For CMMSs-1, i.e. (S)-PSA-based microspheres, they primarily induced L-alanine to form octahedral crystals (Figure 10B) with ee of 62%. To acquire more evidence of the assumption, we further characterized the induced crystals by XRD technique, as shown in **Figure S4** (Supporting Information) by taking L-

alanine as representative. The XRD patterns provide further evidence for our conclusion. The aforementioned results are in well agreement with our earlier studies by using chiral PSA-derived nanoparticles²³ and chiral composite nanoparticles.²⁰ It further reveals that for inducing enantioselective crystallization of alanine enantiomers, PSA (R- and S-PSA) played essential roles by acting as chiral seeds to promoting a certain alanine enantiomer to crystal preferably.

The last point to be highlighted is that the chiral magnetic microspheres could be easily isolated by just using an external magnet. This feature makes the microspheres under investigation advantageous over the non-magnetic counterparts. It also enables the microspheres to be readily recycled. We are currently continuing investigations along this significant direction.

Conclusions

We successfully established a facile and effective approach for preparing chiral, magnetic composite microspheres by performing coordination-precipitation polymerization of acetylenic monomer in the presence of Fe₃O₄ nanoparticles. The microspheres were obtained in high yield (>86 wt%) with regular morphology and high uniformity in size. The composite microspheres possessed both optical activity originated in chiral helical substituted polyacetylene and rapid magnetic responsivity derived from magnetic Fe₃O₄ nanoparticles. The novel microspheres further acted as specific chiral selectors for enantioselective crystallization by using D- and L-alanine as model enantiomers. The coordination-precipitation polymerization is a versatile platform for subsequently preparing novel advanced functional polymer spheres derived from acetylenics, especially for establishing unique composite microspheres.

Acknowledgement.

The project was supported by the “National Natural Science Foundation of China” (21474007, 21274008, 21174010), the Funds for Creative Research Groups of China (51221002), and the “Specialized Research Fund for the Doctoral Program of Higher Education” (SRFDP 20120010130002).

Notes and references

- ^a State Key Laboratory of Chemical Resource Engineering, Beijing University of Chemical Technology, Beijing 100029, China. Fax: +86-10-6443-5128; Tel: +86-10-6443-5128; E-mail: dengjp@mail.buct.edu.cn
- ^b College of Materials Science and Engineering, Beijing University of Chemical Technology, Beijing 100029, China. Fax: +86-10-6443-5128; Tel: +86-10-6443-5128; E-mail: dengjp@mail.buct.edu.cn
- ^c R&D Center of Coal Chemical Industry Company, Shenhua Ningxia Coal Industry Group Co., Ltd, Ningxia, 750411, China.
- 1 J. Liu, J. W. Y. Lam and B. Z. Tang, *Chem. Rev.*, 2009, **109**, 5799–5867.
- 2 J. G. Rudick, and V. Percec, *New J. Chem.*, 2007, **31**, 1083–1096.
- 3 E. Yashima, K. Maeda, H. Iika, Y. Furusho and K. Nagai, *Chem. Rev.*, 2009, **109**, 6102–6211.
- 4 J. G. Kennemur and B. M. Novak, *Israel J. Chem.*, 2011, **51**, 1041–1051.
- 5 M. Shiotsuki, F. Sanda and T. Masuda, *Polym. Chem.*, 2011, **2**, 1044–1058.
- 6 R. P. Megens and G. Roelfes, *Chem. Eur. J.*, 2011, **17**, 8514–8523.
- 7 S. Matsushita and K. Akagi, *Israel J. Chem.*, 2011, **51**, 1075–1095.

- 8 M. M. Green, J. W. Park, T. Sato, A. Teramoto, S. Lifson, R. L. B. Selinger and J. V. Selinger, *Angew. Chem. Int. Ed.*, 1999, **38**, 3138–3154.
- 9 A. R. Palmans and E. W. Meijer, *Angew. Chem. Int. Ed.*, 2007, **46**, 8948–8968.
- 10 Y. Okamoto, *Adv. Polym. Sci.*, 2013, **261**, 391–414.
- 11 R. Wang, X. Li, J. Bai, J. Zhang, A. H. Liu and X. H. Wan, *Macromolecules*, 2014, **47**, 1553–1562.
- 12 N. Suzuki, M. Fujiki, R. Kimpinde-Kalunga and J. R. Koe, *J. Am. Chem. Soc.*, 2013, **135**, 13073–13079.
- 13 L. J. Liu, T. Namikoshi, Y. Zang, T. Aoki, S. Hadano, Y. Abe, I. Wasuzu, T. Tsubata, M. Teraguchi and T. Kaneko, *J. Am. Chem. Soc.*, 2013, **135**, 602–605.
- 14 C. Zhang, H. Wang, Q. Geng, T. Yang, L. Liu, R. Sakai, T. Satoh, T. Kakuchi and Y. Okamoto, *Macromolecules*, 2013, **46**, 8406–8415.
- 15 Y. Yoshida, Y. Mawatari, A. Motoshige, R. Motoshige, T. Hiraoki, M. Wagner, K. Müllen and M. Tabata, *J. Am. Chem. Soc.*, 2013, **135**, 4110–4116.
- 16 R. M. Ho, Y. W. Chiang, S. C. Lin and C. K. Chen, *Prog. Polym. Sci.*, 2011, **36**, 376–453.
- 17 C. Song, X. Liu, D. Liu, C. L. Ren, J. P. Deng and W. T. Yang, *Macromol. Rapid Commun.*, 2013, **34**, 1426–1445; and the references cited therein.
- 18 W. F. Li, H. J. Huang, Y. Li and J. P. Deng, *Polym. Chem.*, 2014, **5**, 1107–1118; and the references cited therein.
- 19 X. F. Luo, J. P. Deng and W. Yang, *Angew. Chem. Int. Ed.*, 2011, **50**, 4909–4912.
- 20 B. Chen, J. P. Deng and W. T. Yang, *Adv. Funct. Mater.*, 2011, **21**, 2345–2350.
- 21 H. Y. Zhang, J. X. Song and J. P. Deng, *Macromol. Rapid Commun.*, 2014, **35**, 1216–1223.
- 22 L. Ding, Y. Y. Huang, Y. Y. Zhang, J. P. Deng and W. T. Yang, *Macromolecules*, 2011, **44**, 736–743.
- 23 D. Y. Zhang, C. Song, J. P. Deng and W. T. Yang, *Macromolecules*, 2012, **45**, 7329–7338.
- 24 D. Liu, L. Zhang, M. Li, W. Yang and J. P. Deng, *Macromol. Rapid Commun.*, 2012, **33**, 672–677.
- 25 L. H. Reddy, J. L. Arias, J. Nicolas and P. Couvreur, *Chem. Rev.*, 2012, **112**, 5818–5878.
- 26 V. Ivanovskaya, L. C. Phillips, A. Zobelli, I. C. Infante, E. Jacquent, V. Garcia, S. Fusil, P. R. Briddon, N. Guiblin, A. Mougin, A. A. Únal, F. Kronast, S. Valencia, B. Dkhil, A. Barth dány and M. Bibes, *Nat. Mater.*, 2014, **13**, 345–351.
- 27 M. N. Moghadama, V. Kolesovb, A. Vogela, H. A. Klok and D. P. Pioletti, *Biomaterials*, 2014, **35**, 450–455.
- 28 K. Ding, L. H. Jing, C. Y. Liu, Y. Hou and M. Y. Gao, *Biomaterials*, 2014, **35**, 1608–1617.
- 29 B. Panella, A. Vargas and A. Baiker, *J. Catal.*, 2009, **261**, 88–93.
- 30 H. Tan, J. M. Xue, B. Shuter, X. Li and J. Wang, *Adv. Funct. Mater.*, 2010, **20**, 722–731.
- 31 S. Balasubramaniam, S. Kayandan, Y. N. Lin, D. F. Kelly, M. J. House, R. C. Woodward, T. G. S. Pierre, J. S. Riffle and R. M. Davis, *Langmuir*, 2014, **30**, 1580–1587.
- 32 F. Zamani and S. Kianpour, *Catal. Commun.*, 2014, **45**, 1–6.
- 33 M. F. Shao, F. Y. Ning, J. W. Zhao, M. Wei, D. Evans and X. Duan, *J. Am. Chem. Soc.*, 2012, **134**, 1071–1077.
- 34 O. Veisheh, J. W. Gunn and M. Zhang, *Adv. Drug Delivery Rev.*, 2010, **62**, 284–304.
- 35 S. C. McBain, H. H. Yiu and J. Dobson, *Int. J. Nanomed.*, 2008, **3**, 169–180.
- 36 A. Hu, G. T. Yee and W. Lin, *J. Am. Chem. Soc.*, 2005, **127**, 12486–12487.
- 37 O. Gleeson, G.-L. Davies, A. Peschiulli, R. Tekoriute, Y. K. Gun'ko and S. J. Cannon, *Org. Biomol. Chem.*, 2011, **9**, 7929–7940.
- 38 S. Ghosh, A. Z. M. Badruddoza, M. S. Uddin and K. J. Colloid Interface Sci., 2011, **354**, 483–492.
- 39 H. J. Choi and M. H. Hyun, *Chem. Commun.*, 2009, **42**, 6454–6456.
- 40 X. Zheng, L. Zhang, J. Li, S. Luo and J.-P. Cheng, *Chem. Commun.*, 2011, **47**, 12325–12327.
- 41 A. P. Kumar, J. H. Kim, T. D. Thanh and Y.-I. Lee, *J. Mater. Chem. B.*, 2013, **1**, 4909–4915.
- 42 R. R. Schrock and J. A. Osborn, *Inorg. Chem.*, 1970, **9**, 2339–2343.
- 43 Z. G. Zhang, J. P. Deng, W. G. Zhao, J. M. Wang, W. T. Yang, *J. Polym. Sci. Part A: Polym. Chem.*, 2007, **45**, 500–508.
- 44 Y. Sun, X. B. Ding, Z. Zheng, Z. H. Zheng, X. Cheng, X. H. Hu and Y. X. Peng, *Eur. Polym. J.*, 2007, **43**, 762–772.
- 45 D. D. Medina, J. Goldshtein, S. Margel and Y. Mastai, *Adv. Funct. Mater.*, 2007, **17**, 944–950.
- 46 Y. Mastai, *Chem. Soc. Rev.*, 2009, **38**, 772–780.
- 47 W. F. Li, X. Liu, G. Y. Qian and J. P. Deng, *Chem. Mater.*, 2014, **26**, 1948–1956.
- 48 J. Park, K. An, Y. Hwang, J. G. Park, H. Noh, J. Y. Kim, J. H. Park, N. M. Hwang and T. Hyeon, *Nat. Mater.*, 2004, **3**, 891–895.
- 49 Y. S. Kang, S. Risbud, J. F. Rabolt and P. Stroeve, *Chem. Mater.*, 1996, **8**, 2209–2211.
- 50 H. Deng, X. L. Li, Q. Peng, X. Wang, J. P. Chen and Y. D. Li, *Angew. Chem. Int. Ed.*, 2005, **117**, 2842–2845.
- 51 J. P. Deng, J. Tabei, M. Shiotsuki, F. Sanda and T. Masuda, *Macromolecules*, 2004, **37**, 1891–1896.
- 52 M. Tabata, T. Fukushima and Y. Sadahiro, *Macromolecules*, 2004, **37**, 4342–4350.
- 53 D. Liu, H. Y. Chen, J. P. Deng and W. T. Yang, *J. Mater. Chem. C.*, 2013, **1**, 8066–8074.
- 54 A. Mukhopadhyay, N. Joshi, K. Chattopadhyay and G. De, *ACS Appl. Mater. Interfaces*, 2011, **4**, 142–149.

The table of contents entry: **Optically active helical polyacetylene/Fe₃O₄ composite microspheres: prepared by precipitation polymerization and used for enantioselective crystallization**

Huaiyu Chen,^{a,b} Lei Li,^{a,b,c} Dong Liu,^{a,b} Huajun Huang,^{a,b} Jianping Deng*^{a,b} and Wantai Yang^{a,b}

The first coordination-precipitation polymerization for constructing chiral, magnetic composite microspheres based on helical substituted polyacetylene and Fe₃O₄ nanoparticles: preparation and their application in enantioselective crystallization

ToC figure

